J|A|C|S
ARTICLES

Published on Web 09/24/2009

Supramolecular Aggregation of Inorganic Molecules at Au(111) Electrodes under a Strong Ionic Atmosphere

Yong-Chun Fu, Yu-Zhuan Su, De-Yin Wu, Jia-Wei Yan, Zhao-Xiong Xie, and Bing-Wei Mao*

State Key Laboratory of Physical Chemistry of Solid Surfaces and Department of Chemistry, College of Chemistry and Chemical Engineering, Xiamen University, Xiamen 361005, China

Received March 25, 2009; E-mail: bwmao@xmu.edu.cn

Abstract: Neutral inorganic molecules are generally weak in surface adsorption and intermolecular interactions. Self-assembly of such types of molecule would provide valuable information about various interactions. At electrochemical interfaces, the relative strength of these interactions may be modified through control of electrode potential and electrolyte, which may lead to the discovery of new structures and new phenomena. However, studies of this nature are as yet lacking. In this work, we consider the covalent-bound semimetal compound molecules, XCl_3 (X = Sb, Bi), as model systems of neutral inorganic molecules to investigate their self-assembly at electrochemical interfaces under a high ionic atmosphere. To fulfill such investigations, *in situ* STM and cyclic voltammetry are employed, and comparative experiments are performed on Au(111) in ionic liquids as well as aqueous solutions with high ionic strength. In the room temperature ionic liquid of 1-butyl-3-methylimidazolium tetrafluoroborate ($BMIBF_4$), potential-dependent partial charge transfer between the Au surface and XCl_3 molecules creates a molecule−surface interaction and provides the driving force for adsorption of the molecules. Supramolecular aggregations of adsorbed XCl_3 are promoted through chlorine-based short-range intermolecular correlation under crystallographic constraint, while repulsive Coulombic interactions created between the partially charged aggregations facilitate their long-range ordering. For $SbCl_3$ molecules, hexagonally arranged 6- or 7-member clusters are formed at 0.08 to −0.2 V (vs Pt), which assemble into a secondary $(\sqrt{31} \times \sqrt{31})R8.9°$ structure. For $BiCl_3$ molecules, both the 6-membered hexagonal and 3-membered trigonal clusters are formed in the narrow potential range −0.3 to −0.35 V, and are also arranged into an ordered secondary structure. Comparative studies were performed with $SbCl_3$ in concentrated aqueous solutions containing 2 M HCl to simulate the strong ionic strength of the ionic liquid. Almost identical 6-/7-member clusters and long-range $(\sqrt{31} \times \sqrt{31})R8.9°$ structure are observed at −0.1 V, demonstrating the crucial role of strong ionic strength in such supramolecular aggregations. However, such supramolecular structures are modified and eventually destroyed as ionic strength is further increased by addition of $NaClO_4$ up to 6 M. The destructive changes of the supramolecular structures are attributed to the alteration of ion distribution in the double layer from cation-rich to anion-rich at increasing $NaClO_4$ concentration. This modifies and eventually breaks the balance of intermolecular and molecule−electrolyte interactions. Finally, the dynamic behavior of the $SbCl_3$ assembly is investigated down to molecular level. It has been demonstrated that the initial stage of assembly follows a two-dimensional nucleation and growth mechanism and has a potential-dependent rate that is closely related to the surface mobility of the $SbCl_3$ clusters. There is a probability that clusters can escape from an existing assembly domain or insert into a vacancy in such a domain while they can also relax with central or ring members in a dynamic fashion. These phenomena indirectly reflect the dynamic properties of cations from electrolytes at the interface. The rich information contained in the self-assembly behavior of $SbCl_3$ and $BiCl_3$ demonstrates that neutral inorganic molecules can be employed for fundamental studies of a variety of interesting issues, especially the interplay of various interfacial interactions.

1. Introduction

The adsorption of molecules and subsequent lateral reorganization are two essential steps in molecular self-assembly at solid surfaces. Accordingly, the delicate balance of molecule−surface and intermolecular interactions leads to an ordered molecular assembly.[1−6] These interactions and the resulting assembly structures can be tuned by varying molecular building blocks, crystallography and temperature of substrates, and working environments. Understanding and control of various interactions and assembling process are important fundamental issues. By using scanning tunneling microscope (STM), investigations in

(1) Love, J. C.; Estroff, L. A.; Kriebel, J. K.; Nuzzo, R. G.; Whitesides, G. M. *Chem. Rev.* **2005**, *105*, 1103.
(2) Wan, L. J. *Acc. Chem. Res.* **2006**, *39*, 334.
(3) Schreiber, F. *Prog. Surf. Sci.* **2000**, *65*, 151.
(4) De Feyter, S.; De Schryver, F. C. *J. Phys. Chem. B* **2005**, *109*, 4290.
(5) Wang, D.; Wan, L. J. *J. Phys. Chem. C* **2007**, *111*, 16109.
(6) Vericat, C.; Vela, M. E.; Salvarezza, R. C. *Phys. Chem. Chem. Phys.* **2005**, *7*, 3258.

10.1021/ja902373q CCC: $40.75

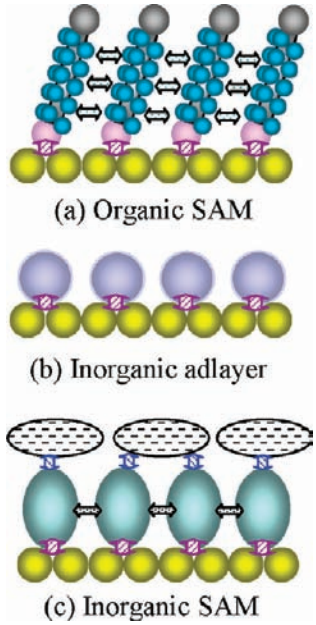

Figure 1. Conceptive diagrams of molecule−surface, molecule−molecule and molecule−electrolyte interactions for (a) organic SAM, (b) inorganic adlayer, and (c) inorganic SAM.

this field have progressed tremendously with expansion of molecular building blocks from thiol-based[1] to heterocyclic aromatic organic molecules[2] as well as of the environments from gas phase,[3] solutions,[4] to electrochemical interfaces.[5] At electrochemical interfaces (i.e., electrode−electrolyte interfaces), the molecule−solution and/or molecule−electrolyte interactions serve as additional factors which together determine assembly structure. A multitude of controls over the aforementioned interactions and dynamics of assembly can be achieved through variation of charge density of the surface and strong electric field across the interface. Therefore, the architectures of molecular assembly structures can be enriched at electrode−electrolyte interfaces.

Depending on the nature of the molecular building blocks, the relative strength of the molecule−surface, molecule−molecule, and molecule−solution interactions can be very different. Organic molecules, which constitute the main body in the field of molecular self-assembly,e.g.[7−13] have various types of functional groups and/or π-electrons, which favor the molecule−surface as well as intermolecular interactions. However, organic molecules are usually neutral with small permanent dipole moments and their interactions with their environment, e.g. molecule−solution interactions, are weak.[5] Hence, self-assembly of these molecules is less sensitive to influence from environment, Figure 1a.

Intensive work has been carried out on the ordered adsorption of inorganic molecular anions such as X^-,[14] CN^-,[15] SO_4^{2-},[16] and $PtCl_4^{2-}$ [17] at electrode−electrolyte interfaces.[14,18,19] These systems are typical of overwhelmingly strong molecule−surface interactions and can only form an adlayer instead of an assembly, because of the lack of lateral reorganization, Figure 1b. Consequently, inorganic molecular anions cannot provide much information about molecule−molecule as well as molecule−electrolyte interactions.

Neutral inorganic molecules are generally weak in surface adsorption and intermolecular interactions because of the lack of functional groups and/or π-electrons, and investigations of the self-assembly of this type of molecule at surfaces are so far scarce. Nevertheless, the molecule−surface interactions in inorganic molecular systems may be promoted through partial charge transfer between the surfaces and molecules at electrode−electrolyte interfaces under potential control, which in turn creates Coulombic interactions between the partially charged molecules and electrolyte ions. As a consequence, self-assembly of neutral inorganic molecules would depend critically on the balance of molecule−surface, molecule−molecule, and molecule−electrolyte interactions, Figure 1c. Therefore, investigations employing neutral inorganic molecules would not only broaden molecular self-assembly to new categories of systems, but also shed light on the balance of various interactions in the control of assembly structure and assembling dynamics.

In this article, we present a systematic *in situ* STM study on the self-assembly of covalently bound semimetal type of inorganic compound molecules on Au(111) by employing $SbCl_3$ and $BiCl_3$ as model systems. Difficulties of working with this type of neutral inorganic molecule in a conventional aqueous solution lie in dissociation and/or hydrolysis processes, which turn the molecules into ionic species. A good strategy is to employ media with high ionic strength so that hydrolysis and dissociation of these inorganic molecules are suppressed. Room temperature ionic liquids are a novel class of solvent composed of e.g. imidazolium cations and weakly coordinating anions, and have found applications in a variety of fields.[20−25] Apart from the wide electrochemical window, the most prominent characteristic of the ionic liquid is the strong ionic atmosphere with lower dielectric constant in comparison with solvent water,[26] which may lead to new structures and phenomena of molecular self-assembly. In a previous study on underpotential deposition of Sb in a room temperature ionic liquid, we have found that $SbCl_3$ can reversibly adsorb at Au(111) electrode surface with formation of a unique long-range ordered structure.[27] By employing *in situ* STM in a series of designed experiments, not only in the room temperature ionic liquid but

(7) Theobald, J. A.; Oxtoby, N. S.; Phillips, M. A.; Champness, N. R.; Beton, P. H. *Nature* **2003**, *424*, 1029.
(8) Cunha, F.; Tao, N. J. *Phys. Rev. Lett.* **1995**, *75*, 2376.
(9) Wan, L. J.; Noda, H.; Wang, C.; Bai, C. L.; Osawa, M. *Chem. Phys. Chem.* **2001**, *2*, 617.
(10) Li, Z.; Han, B.; Wan, L. J.; Wandlowski, Th *Langmuir* **2005**, *21*, 6915.
(11) He, Y. F.; Ye, T.; Borguet, E. *J. Am. Chem. Soc.* **2002**, *124*, 11964.
(12) Zhang, H. M.; Xie, Z. X.; Mao, B. W.; Xu, X. *Chem.—Eur. J.* **2004**, *10*, 1415.
(13) Zhang, H. M.; Yan, J. W.; Xie, Z. X.; Mao, B. W.; Xu, X. *Chem.—Eur. J.* **2006**, *12*, 4006.
(14) Lipkowski, J.; Shi, Z. C.; Chen, A. C.; Pettinger, B.; Bilger, C. *Electrochim. Acta* **1998**, *43*, 2875.
(15) Kim, Y. G.; Yau, S. L.; Itaya, K. *J. Am. Chem. Soc.* **1996**, *118*, 393.
(16) Cuesta, A.; Kleinert, M.; Kolb, D. M. *Phys. Chem. Chem. Phys.* **2000**, *2*, 5684.
(17) Waibel, H. F.; Kleinert, M.; Kibler, L. A.; Kolb, D. M. *Electrochim. Acta* **2002**, *47*, 1461.
(18) Kolb, D. M. *Angew. Chem., Int. Ed.* **2001**, *40*, 1162.
(19) Magnussen, O. M. *Chem. Rev.* **2002**, *102*, 679.
(20) Buzzeo, M. C.; Evans, R. G.; Compton, R. G. *Chem. Phys. Chem.* **2004**, *5*, 1106.
(21) Kornyshev, A. A. *J. Phys. Chem. B* **2007**, *111*, 5545.
(22) Zein El Abedin, S.; Endres, F. *Acc. Chem. Res.* **2007**, *40*, 1106.
(23) Hapiot, P.; Lagrost, C. *Chem. Rev.* **2008**, *108*, 2238.
(24) Lin, L. G.; Wang, Y.; Yan, J. W.; Yuan, Y. Z.; Xiang, J.; Mao, B. W. *Electrochem. Commun.* **2003**, *5*, 995.
(25) Zhou, X. S.; Wei, Y. M.; Liu, L.; Chen, Z. B.; Tang, J.; Mao, B. W. *J. Am. Chem. Soc.* **2008**, *130*, 13228.
(26) Wakai, C.; Oleinikova, A.; Ott, M.; Weingärtner, H. *J. Phys. Chem. B* **2005**, *109*, 17028.
(27) Fu, Y. C.; Yan, J. W.; Wang, Y.; Tian, J. H.; Zhang, H. M.; Xie, Z. X.; Mao, B. W. *J. Phys. Chem. C* **2007**, *111*, 10467.

also in aqueous solutions with unusually high ionic strength, we show in this paper that long-range ordered flower-like supramolecular structures are characteristic of both $SbCl_3$ and $BiCl_3$ molecular assembly, which are consequences of balanced molecule−surface, molecule−molecule, and molecule−electrolyte interactions. Dynamic behavior of $SbCl_3$ assemblies is also followed at molecular level. The results reveal the roles of both electrode and electrolyte sides of the interfaces in precise control of the various interactions.

2. Experimental Section

A series of experiments were designed to modify the strength of various interactions: First, 1-butyl-3-methylimidazolium tetrafluoroborate ($BMIBF_4$) was employed, a room temperature ionic liquid in which $SbCl_3$ and $BiCl_3$ molecules maintain molecular structure. The structures of assemblies of both molecules were characterized by *in situ* STM to verify its generality. Next, to probe the media influence, comparative studies were carried out in solutions in concentrated hydrochloric acid, in which hydrolysis of the molecules is suppressed and their structures are maintained. To inspect the influence of ionic strength, the concentration of these aqueous solutions was further varied by addition of very concentrated $NaClO_4$ as supporting electrolyte. Finally, the dynamic behavior of $SbCl_3$ assembly is monitored at molecular level in both ionic liquid and aqueous solutions.

Synthesis of $BMIBF_4$ has been described in a previous paper.[27] Special attention has been paid to each step of the procedure to ensure the highest possible purity. The prepared ionic liquid is colorless or pale yellow, which gives a relatively simple CV without obvious current response in a wide electrochemical window (Figure S1, Supporting Information). Solutions were prepared by dissolving $SbCl_3$ or $BiCl_3$ (Alfa, 99.999%) in the $BMIBF_4$ ionic liquid with concentration typically at 0.01 M. Prior to each measurement, the salt-containing $BMIBF_4$ solution was dried in vacuum at 70 °C for several hours to remove absorbed water, and experiments were conducted under protection of N_2 atmosphere.

Au(111) surfaces were obtained from single-crystal beads.[28] For *in situ* STM measurements, one of the (111) facets of the bead was used directly, whereas for electrochemical measurements the single-crystal bead was oriented and polished to expose a large enough (111) plane. Prior to each experiment, the working surface was subjected to electrochemical polishing and flame annealing in H_2 followed by cooling under N_2 atmosphere.

In situ STM measurements were carried out on Nanoscope IIIa STM instrument (Digital Instruments, Santa Barbara, CA) under constant-current mode in a nitrogen atmosphere. STM tips were prepared by mechanically cutting Pt−Ir wires (0.25 mm in diameter) followed by insulating by thermosetting polyethylene to reduce the Faradaic current. Cyclic voltammetric measurements were performed on a CHI electrochemical workstation (CHI Instruments, Austin, TX). For both electrochemical and STM measurements, platinum wires were used as the counter and quasi-reference electrodes, respectively. All of the potentials reported in this paper are versus Pt quasi-reference electrode, unless otherwise stated. All bias voltages for STM imaging are given in a tip vs sample convention.

3. Results and Discussion

3.1. Supramolecular Aggregation in Ionic Liquids. $SbCl_3$ and $BiCl_3$ are neutral molecules having a pseudotetrahedral type of structure with the three Cl atoms and the electron lone pair from the metal occupying the four apical sites. The molecules have a large dipole moment of 3.5 D for $SbCl_3$ and 4.5 D for $BiCl_3$ as calculated by hybrid density function theory (DFT). (See also ref 29.) Raman spectroscopic studies on molten XCl_3, where X denotes Sb or Bi, have indicated that these molecules exist with molecular structure maintained.[30,31] Recent molecular dynamics simulation on the solvation of $LaCl_n^{3-n}$ complexes in the $BMIBF_4$ ionic liquid reveals that all complexes with up to six chlorides remain bound although noncovalent, mainly steric and electrostatic, cation−anion interactions influence the final orientation.[32]

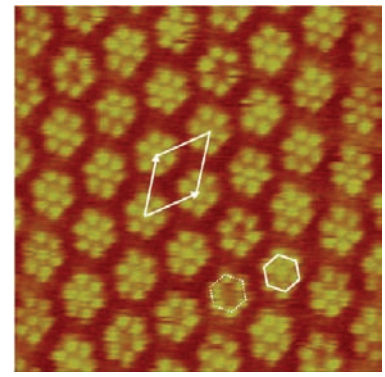

Figure 2. Ordered array of supramolecular structures of $SbCl_3$ on Au(111) in the $BMIBF_4$ containing 0.01 M $SbCl_3$ in the potential range 0.08 to −0.2 V. Scan size: 10 nm × 10 nm. Tunneling current: 1 nA. Bias voltage: 100 mV.

Considering the covalent-bound nature of XCl_3 as well as the lower dielectric constant of ionic liquids (∼11 for $BMIBF_4$[26]), it is reasonable to assume that XCl_3 maintain their molecular structure when dissolved in the $BMIBF_4$ ionic liquid. These small molecules are weak in intermolecular interactions because of the lack of sufficient van der Waals interactions, hydrogen bonding, and $\pi-\pi$ interactions. Nevertheless, $SbCl_3$ and $BiCl_3$ have empty 5d and 6d electron orbitals, respectively, and partial charge transfer from the surface to the molecules is thus possible, which favors molecule−surface interactions though much weaker than those in the molecular anion systems. It is expected that self-assembly of these molecules in ionic liquids would be strongly dependent on the interactions from both sides of the electrode−electrolyte interfaces.

3.1.1. Supramolecular Structure of $SbCl_3$. *In situ* STM characterization reveals that $SbCl_3$ molecules can assemble on a Au(111) electrode in ionic liquids upon a cathodic excrusion between 0.08 to −0.2 V, which is well before the onset of underpotential deposition (UPD) of Sb.[27] A hexagonally arranged cluster array is formed as shown in Figure 2. Each cluster is composed of hexagonally arranged 6 or 7 members with the 6-membered clusters taking a much smaller fraction (∼18%) at equilibrium. Dynamic on or off events of the central members are observed (*vide infra*). Each member of the cluster has a spherical appearance in the STM image with diameter of 0.36 nm and corrugation height of 0.05 nm. The array has the nearest cluster distance of 1.61 nm, while the cluster has the nearest spot distance of 0.43 nm. Change of bias voltage does not lead to change of the characteristics of the STM images. A unit cell of the array corresponding to a Au(111)($\sqrt{31} \times \sqrt{31}$)R8.9° structure is highlighted on the image. The small cluster size in

(28) Clavilier, J.; Armand, D.; Sun, S. G.; Petit, M. *J. Electroanal. Chem.* **1987**, *205*, 267.
(29) Homma, H.; Clarke, R. *Phys. Rev. B* **1985**, *31*, 5865.
(30) Fung, K. W.; Begun, G. M.; Mamantov, G. *Inorg. Chem.* **1973**, *12*, 53.
(31) Okamoto, Y.; Yaita, T.; Minato, K. *J. Mol. Struct.* **2005**, *749*, 70.
(32) Chaumont, A.; Wipff, G. *J. Phys. Chem. B* **2004**, *108*, 3311.

comparison with the large periodicity of the cluster array provides a rationality to regard the cluster as a supramolecular structure. The phenomenon is distinct from that reported in typical sulfuric acid solutions containing Sb(III),[33−35] where irreversible adsorption of oxygeneous SbO^+ is the main feature.[36,37]

Clearly, the apparent spot size (0.36 nm) is not equivalent to the real covalent diameter of Sb (0.282 nm). Control experiments showed no cluster formation in the potential region employed, which excludes the possibility of adsorption from the cation (BMI^+) or anion (BF_4^-) of the ionic liquid. In addition, complete or partial discharge of Sb(III) to elemental Sb(0) is not possible in this potential range based on the estimation of charge flux associated with the cluster formation (~40 $\mu C \cdot cm^{-2}$, Figure S2, Supporting Information). Furthermore, since the clusters are formed upon cathodic potential excursions, only the adsorption of $SbCl_3$ molecules becomes possible after having excluded the adsorption of BMI^+ cations in the control experiment. Such a molecule-related nature of spots in the clusters is supported by the necessity of crystallographic matching between the molecules and surface, which has been proved by the absence of clusters in the $SbBr_3$-containing ionic liquid in separate experiments.[38]

On the basis of the above facts, the spots in the clusters can be attributed to individual $SbCl_3$ molecules. The simplex spherical appearance of the spots indicates a symmetric projection of the molecules, implying that the three chlorines of $SbCl_3$ would be in either an up or down configuration. It follows that the Au(111)($\sqrt{31} \times \sqrt{31}$)R8.9° structure corresponds to a fractional coverage of ~7/31 of the $SbCl_3$ molecules.

The observed supramolecular $SbCl_3$ clusters have similarities with the hollow hexagonal CN^- rings on Pt(111) observed by Itaya and co-workers.[15] However, the major difference between these two systems is that CN^- is an extremely strong adsorbing anion with poor tunability by potential and solution ionic strength. Different levels of dynamic behavior cannot be observed for the adsorbed CN^- adlayer, (*vide infra*).

3.1.2. Supramolecular Structure of $BiCl_3$. The above-observed supramolecular aggregation appears to be a general phenomenon of the assembly of semimetal trichloride compound molecules. To examine this point, the assembly of $BiCl_3$ on Au(111) was investigated. In the $BMIBF_4$ ionic liquid, $BiCl_3$ molecules also form long-range ordered supramolecular structures within a narrower potential range upon cathodic potential excursion to −0.3 V, which is just before the onset of Bi UPD at −0.38 V (Figure S3, Supporting Information). As shown in Figure 3a, the assembly has a complex structure that is composed of two sets of clusters, namely 6-membered hollow hexagonal clusters and 3-membered trigonal clusters, wherein each of the 6-membered clusters is surrounded by six trigonal clusters. The periodicity of the hexagonally arranged 6-membered clusters is 2.90 nm, corresponding to a commensurate Au(111)(10 × 10) structure. Each spot in the clusters takes a diameter of 0.5 nm with a corrugation height of 0.14 nm, which

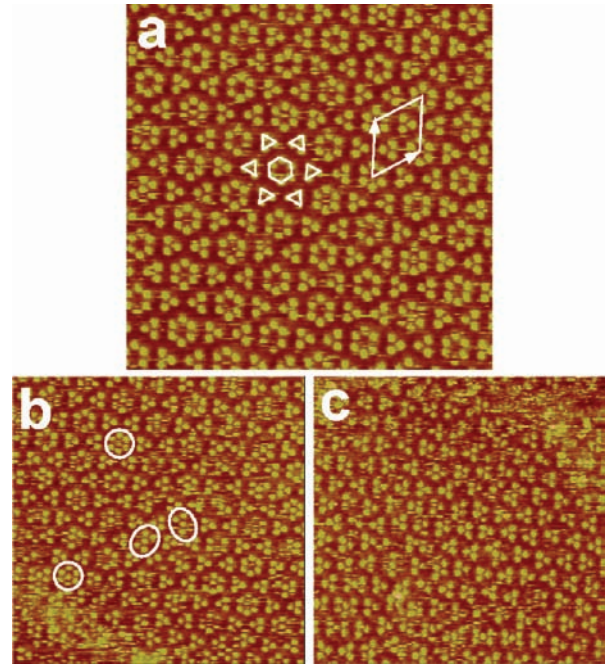

Figure 3. (a) Ordered arrays of $BiCl_3$ clusters on Au(111) surface in $BMIBF_4$ ionic liquid containing 0.01 M $BiCl_3$ at −0.3 V. (b, c) Structural transformation of the $BiCl_3$ clusters upon potential decrease to −0.35 V; (c) was recorded several minutes after (b). Scan size: 20 nm × 20 nm. Tunneling current: 1 nA. Bias voltage: 400 mV.

is much larger than the diameter of a Bi atom (0.326 nm). Again, these structural features are distinct from those observed in aqueous solutions containing Bi(III).[39,40] By the same principle, the spots can be proved to be individual $BiCl_3$ molecules as for $SbCl_3$. Noteworthy is the short scratching lines across the clusters on the STM images, meaning the adsorbates are to some extent mobile under the STM scanning tip. Interestingly, decrease of potential to −0.35 V results in a structural transformation through various intermediate stages as marked by oval circles in Figure 3b. Eventually, only the trigonal clusters are preserved on the entire surface in a less regularly arranged manner, Figure 3c.

The above results have demonstrated that neutral inorganic molecules can form surface-assembled monolayers in an ionic liquid under appropriate potential control. Both $SbCl_3$ and $BiCl_3$ form SAMs with two levels of structure, namely, the supramolecular structures and long-range ordered arrays of the supramolecular structures.

3.2. Supramolecular Aggregation of $SbCl_3$ in Aqueous Solutions. Strong ionic strength is one of the most prominent characteristics of ionic liquids. Molecule−electrolyte interactions under such strong ionic strength are likely to be in a delicate balance with other interactions to promote the supramolecular aggregation of XCl_3 and long-range ordering. To explore this assessment, we performed measurements focused on $SbCl_3$ employing aqueous solutions, whose ionic strength is as strong as that of the ionic liquid, yet adjustable by further addition of supporting electrolytes. For this purpose, a 2 M HCl solution is used as the solution, in which the hydrolysis of $SbCl_3$ (~0.017 M) is suppressed (see Note S1 in the Supporting Information).

(33) Wu, Q.; Shang, W. H.; Yan, J. W.; Mao, B. W. *J. Mol. Catal. A* **2003**, *199*, 49.
(34) Jung, C.; Rhee, C. K. *J. Phys. Chem. B* **2005**, *109*, 8961.
(35) Jung, C.; Rhee, C. K. *J. Electroanal. Chem.* **2004**, *566*, 1.
(36) Feliu, J. M.; Fernandez-Vega, A.; Aldaz, A.; Clavilier, J. *J. Electroanal. Chem.* **1988**, *256*, 149.
(37) Climent, V.; Herrero, E.; Feliu, J. M. *Electrochimi. Acta* **1998**, *44*, 1403.
(38) Fu, Y. C.; Zhang, H. M.; Su, Y. Z.; Wu, D. Y.; Xie, Z. X.; Mao, B. W. *Z. Phys. Chem.* **2007**, *221*, 1.
(39) Chen, C. H.; Gewirth, A. A. *J. Am. Chem. Soc.* **1992**, *114*, 5439.
(40) Chen, C. H.; Kepler, K. D.; Gewirth, A. A.; Ocko, B. M.; Wang, J. *J. Phys. Chem.* **1993**, *97*, 7290.

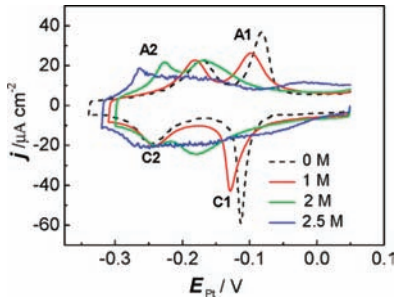

Figure 4. CVs of Au(111) in aqueous solutions of 2 M HCl + 0.017 M $SbCl_3$ with various concentrations of $NaClO_4$. Scan rate: 50 mV s^{-1}.

One of the advantages of working with aqueous solutions over ionic liquids is that the former have much lower viscosity and thus a higher diffusion coefficient. This allows more accurate estimation of the charge flux associated with the adsorption process. Figure 4 shows a set of cyclic voltammograms (CVs) of Au(111) in the $SbCl_3$-containing solutions of varying ionic strengths, which were recorded in the potential region well before the electrodeposition of Sb. As can be seen from the CV in the solution free of $NaClO_4$ (black line), two well-defined couples of capacitive peaks C1(−0.113 V)/A1(−0.082.V) and C2(−0.247 V)/A2(−0.172 V) are obvious with peak separation ($\Delta V_P = V_{PA} - V_{PC}$) of 31 and 75 mV and associated charge flux of ∼21.1 and ∼15.3 $\mu C \cdot cm^{-2}$, respectively. These values are much smaller than the value required to reduce Sb(III) to Sb(0) in a full coverage, which is equivalent to roughly 660 $\mu C \cdot cm^{-2}$. Even given the fractional coverage of ∼7/31 (*vide supra*), only partial charge transfer is possible in association with the adsorption. We stress that peak C1 has a narrow width, which may well be the result of an ion-pairing effect by which the partially charged adsorbates, $SbCl_3$ clusters, would be stabilized by counterions from the solution side, in favor of the adsorption kinetics.[41] Specifically, a layer of cations is expected to locate in the close vicinity of the partially and negatively charged $SbCl_3$ clusters at the surface.

However, further increase of the ionic strength with addition of $NaClO_4$ modifies the CV. With 1 M $NaClO_4$ (red line), the C1/A1 couple shifts only slightly in the cathodic direction with a slight reduction in peak height. When the $NaClO_4$ concentration is increased to 2 M, substantial changes occur (green line): the C1/A1 couple is dramatically shifted and broadened with reduced peak height, partially overlapping with the C2/A2. More remarkably, further increase of $NaClO_4$ concentration to 2.5 M, the C1/A1 couple disappears almost completely. Regardless of all these changes, C2 remains almost unchanged in potential and shape. These characteristics of CVs contain important information that as the ionic strength of the system is increased above the critical value of 2 and 2.5 M, respectively, the nature of the interactions at the interface is changed dramatically, very likely from Coulombic attraction to repulsion when an ion-paring effect no longer exists.

The concentration-dependent voltammetric behavior can be understood with structural association by *in situ* STM measurements in corresponding solutions. In 2 M HCl solution containing $SbCl_3$, following a cathodic potential excursion, STM images show two successive assembling processes associated with peaks C1 and C2, respectively, i.e. the formation of a ($\sqrt{31} \times \sqrt{31}$)R8.9° array structure of the supramolecular clusters (Figure 5a) and the phase transition to form a more closely packed ($\sqrt{19} \times \sqrt{19}$) R23.4° array structure (Figure 5b), respectively. Surprisingly, the supramolecular structure in the ($\sqrt{31} \times \sqrt{31}$)R8.9° array structure has almost exactly the same features as those observed in the ionic liquid, Figure 5a. The periodicity of the clusters, neighboring distance, and size of the spots within the clusters are almost identical to those in the ionic liquid (refer to Figure 2). Correlating the structure with the charge flux associated with peak C1 reveals an average partial charge transfer of ∼2.6 electrons per 7-membered $SbCl_3$ cluster. The ($\sqrt{19} \times \sqrt{19}$) R23.4° structure, which is absent in the ionic liquid, has features similar to those of the ($\sqrt{31} \times \sqrt{31}$)R8.9° structure, but cluster density in the ($\sqrt{19} \times \sqrt{19}$) R23.4° structure is about 63.2% higher. The charge flux of 15.3 μC cm^{-2} associated with peak C2 is roughly equivalent to the amount required to host the additional 6-/7-member clusters with the same charge state.

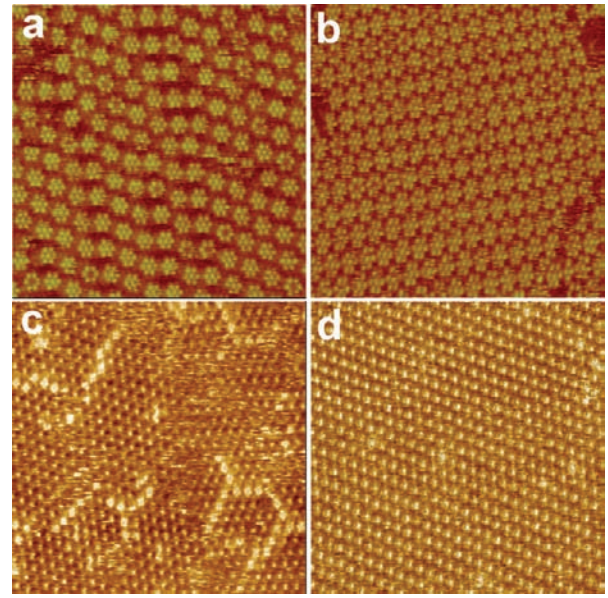

Figure 5. *In situ* STM images of Au(111) in aqueous solutions of 2 M HCl + 0.017 M $SbCl_3$ with varying concentrations of $NaClO_4$. (a) ($\sqrt{31} \times \sqrt{31}$)R8.9° structure of loosely packed $SbCl_3$ cluster array at −0.1 to −0.15 V. (b) ($\sqrt{19} \times \sqrt{19}$)R23.4° structure of densely packed $SbCl_3$ clusters at −0.3 V. (c, d) Adsorption of simplex individual $SbCl_3$ molecules with additionally added $NaClO_4$ at 2 M (c) and 2.5 M. (d) Scan size: 20 nm × 20 nm. Tunneling current: 6−8 nA. Bias voltage: 0.6−0.85 V.

The common feature of the 6-/7-member clusters and ($\sqrt{31} \times \sqrt{31}$)R8.9° array structure observed in the two very different media, $BMIBF_4$ ionic liquid and concentrated HCl solution, implies the same origin of supramolecular aggregation, which can only be attributed to the strong ionic strength of the electrolytes. However, as ClO_4^- concentration is increased to 2 M, the clusters and ($\sqrt{31} \times \sqrt{31}$)R8.9° array structure disappear. Instead, an ordered adlayer with simplex structure appears, Figure 5c, although a small fraction of 4-membered square clusters of $SbCl_3$ can still coexist at this concentration. With further increase of the ClO_4^- concentration to 2.5 M, an ordered ($\sqrt{7} \times \sqrt{7}$) structure appears entirely on the surface, Figure 5d, each spot corresponding to one individual $SbCl_3$ molecule. More dramatically, as the ClO_4^- concentration reaches ∼6 M (Figure S4, Supporting Information), all of the ordered structures are destroyed, and the STM images look featureless. These distinct changes in the structure of $SbCl_3$ assembly have a similar relationship to $NaClO_4$ concentration with the changes in CVs.

(41) Xing, X. K.; Bae, I. T.; Scherson, D. A. *Electrochim. Acta* **1995**, *40*, 29.

The cause of the destructive change of $SbCl_3$ cluster structure in aqueous solutions is considered to be related to the alteration of double layer structure of the electrified interface. At increasingly high concentrations of $NaClO_4$, most of the water molecules would be required to solvate Na^+ cations, leaving ClO_4^- anions less solvated or even naked. The Coulombic repulsions thus created between the naked ClO_4^- on the solution side and the negatively charged $SbCl_3$ clusters on the electrode side are an unfavorable factor which eventually disrupts supramolecular aggregation. The dramatic broadening and severe distortion of CVs at increasing concentration of $NaClO_4$ (Figure 4) are also results of such change in double layer structure. Obviously, the Coulombic repulsions become sufficiently strong at $NaClO_4$ concentration of ~6 M to prevent the formation of any ordered structure of $SbCl_3$. Under these conditions, competitive adsorption of ClO_4^- cannot be excluded either.

3.3. Origin of Supramolecular Structures. The question of whether these clusters already exist in solution is difficult to address because of the lack of techniques. However, such a possibility may excluded for two reasons: (i) the concentrations of $SbCl_3$ and $BiCl_3$ in ionic liquid and in aqueous solutions seem too low for molecules to encounter and form clusters; (ii) on Au(100), adsorption of $SbCl_3$ is not seen,[27,38] while $BiCl_3$ appears as individual molecules (Figure S5, Supporting Information).

As has been demonstrated above, the self-assembly of XCl_3 forms two levels of structures: the primary supramolecular cluster structure which employs individual molecules as building blocks and the secondary cluster array structure which employs the supramolecular clusters as building blocks. For convenience of discussion, proposed models are given for the primary supramolecular structures of XCl_3. All molecules are assumed to adsorb at the three-fold hollow sites with the chlorine atoms orientated in an upward direction.

For the 6-/7-membered $SbCl_3$ clusters, the measured distance between the neighboring spots is 0.43 nm. This value is slightly smaller than the closest possible distance between two individual $SbCl_3$ molecules. An intriguing question is how the two $SbCl_3$ molecules are accommodated within a limited space. Here we mention that X-ray and neutron diffraction patterns have indicated that molten trivalent metal halides have strong intermolecular correlation.[42] In the case of molten $SbCl_3$, each Sb atom has three chlorine neighbors from other molecules to form a distorted octahedral arrangement. Borrowing its molten state properties, a possible interpretation for the apparently crowded arrangement of $SbCl_3$ cluster would be the strong correlation of chlorine atoms of neighboring molecules at the surface under crystallographic constraint. Under this circumstance, the Cl−Cl distance within the $SbCl_3$ molecule has to be shortened with reduced Cl−Sb−Cl dihedral angles. Alternatively, the six $SbCl_3$ molecules could also take an antiparallel arrangement, i.e. three $SbCl_3$ molecules that are located at every other position of the hexagonal cluster take the Sb-down configuration while the other three $SbCl_3$ molecules take the Sb-up configuration. While such an antiparallel arrangement could create an attractive antiparallel dipole−dipole intermolecular interaction, the molecule−surface interaction with the Sb-up configuration would become less effective. In addition, such an antiparallel arrangement would be expected to give two sets of tunneling maxima corresponding to the Sb-up and the Sb-down configuration, respectively, which is however in violation of the observed apparently simplex tunneling spots of the STM images. The origin of the crowded arrangement of $SbCl_3$ within the cluster and long-range order of the clusters deserve elaborate theoretical investigation.

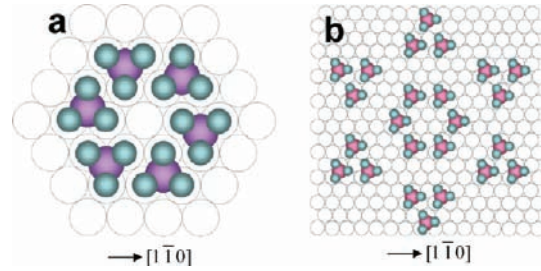

Figure 6. Proposed models for the 6-membered hexagonal clusters of $SbCl_3$ (a) and hexagonal and trigonal clusters of $BiCl_3$ (b).

For the hexagonal and trigonal $BiCl_3$ clusters, the nearest neighbor spot distance of 0.60 nm in the STM image is sufficiently large to accommodate two $BiCl_3$ molecules in a parallel arrangement perpendicular to the surface. The molten salt state of $BiCl_3$ also has a strong tendency to interact intermolecularly to allow for relatively fast exchange of halogen ions.[42] Correlation of chlorine atoms of the neighboring $BiCl_3$ molecules within the cluster is also regarded as the origin of the intermolecular interaction. With the parallel arrangement of the XCl_3 molecules in the clusters, the chlorine-based intermolecular interaction would have to be much stronger than the repulsive dipole−dipole interactions between molecules to enable supramolecular aggregation.

Another fact is that the 6- or 7-membered clusters of $SbCl_3$ always coexist within the potential region of inspection (0.08 to −0.2 V). We therefore expect the 6- or 7-membered cluster structures to have only marginally small energy differences determined by the central member. In view of the observed dynamic behavior of the central members (*vide infra*), it is reasonable to consider that the coexistence of the 6- and 7-membered results from motion of solution species (cations) in the vicinity which determine the presence or absence of the less stable central members. In other words, taking into account the contribution of molecule−solution interaction, the total energy of individual clusters should remain the same, regardless of 6- or 7-membered clusters.

Regarding the hexagonal cluster of $BiCl_3$, the space left in the center would be sufficient to accommodate a seventh $BiCl_3$ molecule in the cluster. The apparent absence of the member in the center may imply fast dynamic behavior, which can be sensed by the short scratching lines in the central part of the clusters on the STM images (refer to Figure 3a). On the other hand, the coexistence of trigonal clusters for $BiCl_3$ is considered to play a role in the minimization of the total energy of the system. The stability of the hexagonal and trigonal $BiCl_3$ clusters can be compared from the correlation among the chlorine atoms according to Figure 6. In the case of hexagonal clusters, each $BiCl_3$ molecule interacts with two neighboring $BiCl_3$ molecules involving 4 Cl−Cl correlations. In the case of trigonal clusters, each $BiCl_3$ molecule also interacts with two neighboring $BiCl_3$ molecules but with each cluster involving total 6 Cl−Cl correlations. This explains the potential-induced transformation from the hexagonal clusters to more closely packed trigonal clusters upon cathodic potential excursion. However, for both the hexagonal and trigonal clusters, each cluster has an average of 2 Cl−Cl correlations per $BiCl_3$ molecule. Therefore, the energy difference between the two structures is expected to be

(42) Tosi, M. P. *J. Phys.: Condens. Matter* **1994**, *6*, A13.

very small. Furthermore, since the supramolecular aggregation is fulfilled at the surface under crystallographic constraints, their precise stability should also be related to the crystallography of the substrate, electrode potential and molecule−electrolyte interaction. In particular, the synergetic effect of electrolyte such as electrostatic balance by the counterions (cations) from the electrolyte side cannot be underestimated for the whole system to reach an energy minimum.

Summarizing the XCl_3 self-assembly on Au(111), the synergistic effects of molecule−surface, molecule−molecule, and molecule−electrolyte interactions are indispensable for the formation of the observed supramolecular clusters and their array structures. First, adsorption of XCl_3 molecules requires a chemical-nature partial charge transfer from the surface to the empty d orbitals of Sb and Bi. To favor such a charge transfer, the XCl_3 molecules would most likely take the orientation with the metal atoms facing toward the surface. Then, intermolecular interaction is built up via correlation of the neighboring chlorine atoms of the surface bound molecules. Meanwhile, the partially negatively charged XCl_3 molecules create repulsive Coulombic interactions, which favor the establishment of long-range order of the clusters. Finally, the subtle balance of molecule−molecule and molecule−electrolyte interactions plays a crucial role in stabilizing the supramolecular structures of XCl_3 molecules. The molecule−electrolyte interaction is sensitive to the charge state on both sides of the metal−electrolyte interface. Variation of the surface charge density or the ionic strength of the electrolyte modifies the molecule−electrolyte interaction and thus stabilizes or destabilizes the supramolecular structures. The similarities in the supramolecular aggregation of XCl_3 in the ionic liquid as well as the common features of the $SbCl_3$ clusters in the ionic liquid and the concentrated aqueous solutions reveal the generality of supramolecular aggregation of the semimetal type of compound inorganic molecules under properly strong ionic atmosphere.

3.4. Dynamics of Assembly and the Assembled Structure of $SbCl_3$. The dynamics of molecular assembly contains rich information. Particularly, the assembly process at the initial stage requires critical balance between various interactions to build up a stable domain of molecular assembly. From a mechanistic point of view, molecular assembly involves two basic processes: two-dimensional nucleation to form stable nuclei and growth of the nuclei through incorporation of new molecules. The rate to form a critical nucleus depends on the probability of encounter of the adsorbed molecules, which is related to the arrival rate and the surface mobility of the molecules. These factors may sensitively be influenced by potential as well as nature of the electrolytes.

Work devoted to the dynamics of molecular assembly is rather limited.[11,43,44] Borguet and co-workers have studied potential modulated surface mobility and its influence on the formation of ordered self-assembly of porphyrin.[11] However, to the best of our knowledge, there is no report so far on the direct observation of the very initial stage of assembling. The reasons may be as follows: STM is a slow technique with time resolution of seconds so that most molecular assembly processes appear to be too fast to be monitored. Even for systems with slower dynamics, determination of critical size of nuclei, which relies on a sequence of STM images of focused area that includes sufficient number of nuclei and with adequate resolution, remains a great challenge. Since ionic liquids have much higher viscosity than water, it is expected that the assembling process of XCl_3 will be slow at properly selected potentials. This makes it feasible to follow the very initial stage of the assembly process by *in situ* STM. Taking $SbCl_3$ as a model system, we present our studies on the dynamic behavior of molecular assembly in ionic liquid with comparisons made in aqueous solutions. The rich information contained in this system will lead to a comprehensive understanding of the mechanism of molecular self-assembly.

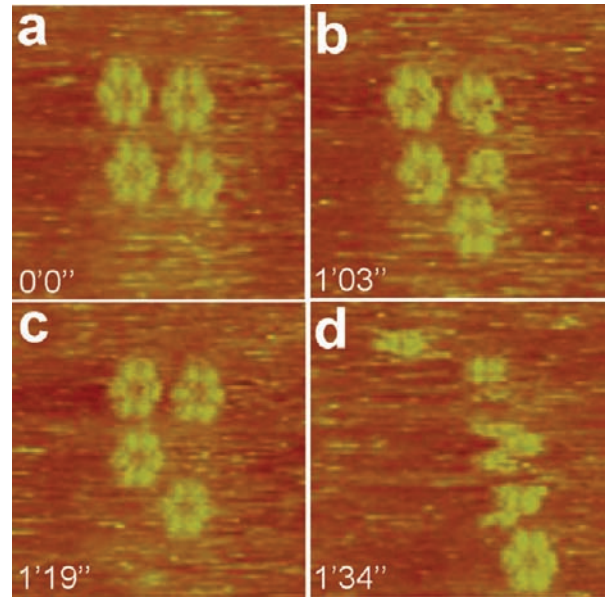

Figure 7. Snapshots of the formation and dissociation of $SbCl_3$ cluster embryos at 50 mV. Solution: $BMIBF_4$ containing 0.01 M $SbCl_3$. Scan size: 7 nm × 7 nm. Tunneling current: 800 pA. Bias voltage: 146 mV.

3.4.1. Nucleation and Growth. In the ionic liquid, assembly of the $SbCl_3$ cluster array structure occurs within a potential range of 80 to −200 mV, in which the 6-/7-membered supramolecular $SbCl_3$ clusters appear as building blocks. Snapshots of the formation and dissociation of several such clusters were captured at the very initial stage at a sufficiently positive potential where the probability for nucleation is low and the balance of various interactions has not been fully established (Figure 7). Four clusters, which have 6-membered configuration, combine to form a nucleus, and this is followed by fast attachment of new clusters and dispersal of existing clusters and finally dissociation of the nucleus. The attachment−detachment behavior reveals the dynamic response of the assembly to unbalanced interactions at a given potential.

The potential dependency of the adsorption rate of $SbCl_3$ is studied by following the rate of formation and coverage of a near-stable assembly domain at different potentials. To fulfill this purpose, an initial potential of 80 mV is applied, which is followed by stepwise cathodic excursions at intervals of 10 mV to a specified potential. STM observations are focused on an appropriate area which includes a sufficient number of nuclei with identifiable clusters. It has been shown that the adsorption rate depends strongly on potential in the initial potential range of 70−30 mV. (Refer to Figure S6 in the Supporting Information.) At the positive end of potential for adsorption, 70 mV, clusters have very high surface mobility as is indicated by the dragging tracks on the STM images. Nucleation appears in a dynamic equilibrium with new nuclei being formed while the existing nuclei subside or dismiss. In other words, there are no critical nuclei which would otherwise develop into reasonably

(43) Berner, S.; Brunner, M.; Ramoino, L.; Suzuki, H.; Gütherodt, H. J.; Jung, T. A. *Chem. Phys. Lett.* **2001**, *348*, 175.
(44) Wakayama, Y.; Hill, J. P.; Ariga, K. *Surf. Sci.* **2007**, *601*, 3984.

Table 1. Potential Dependency of Rate and Coverage of $SbCl_3$ Adsorption

E /mV	time /s	coverage[a] /%
70	−	8.9
60	∼200	34.9
50	∼80	68.9
30	<60	59.0

[a] Calculation of the coverage is based on the model given in Figure 6a as a percentage of adsorbed out of the maximum possible number of $SbCl_3$ molecules.

stable domains. As a consequence, the density of dynamic nuclei is very limited and coverage is low. However, the rate of adsorption can be enhanced at decreasing potential because of increasingly larger driving force for the partial charge transfer of $SbCl_3$. At potentials less than 50 mV, several minutes are sufficient for the adsorption to reach high coverage, while at potentials less than 30 mV, the adsorption process is too fast to be followed. In fact, domains formed at 30 mV are arranged in a relatively disordered way because of fast nucleation on a large scale yet with slower surface mobility. A consequence of this disordered arrangement of clusters is the coverage of the clusters lower even than that seen at 50 mV. The results are summarized in Table 1. We note, however, that large domains can be obtained at $\leq$30 mV provided that the surface is brought to the potential after the formation of an assembly at more positive potentials such as 50 mV. In addition, the dissolution of the as-formed assembly requires anodic overpotential of several tens of millivolts.

To determine the size and geometry of critical nuclei, a potential of 60 mV was selected because the rate of nucleation and growth at this potential is appropriate for STM observation. The most direct approach to determine the critical nuclei would be to acquire a sequence of good-quality STM images, which include at least two successive images that show events of both losing and gaining of clusters from different nuclei that differ in size by only one cluster. In practice, the probability of success with such a requirement is low. Alternatively, the same can be achieved by monitoring the dynamic behavior of nuclei and searching for the smallest stable nuclei during the formation of the assembly structure. The latter is based on the fact that an existing nucleus can either grow or subside/dismiss with time in a certain probability, depending on its geometry and potential. The smallest nuclei that *definitely grow bigger* would give an *upper limit* of the critical size of nuclei, while the largest nuclei that *subside* or *dismiss* would give a *lower limit* of the critical size of nuclei.

Focusing on nuclei which have close-packed configurations, isolated 3- and 6-cluster triangles, 4- and 6-cluster quadrangles, 5-cluster trapezias (Figure 8a and b, highlighted in thick colors) and nearly isolated 7-cluster hexagons (Figure 8d and e, highlighted in thick white) are found to form as the smallest nuclei in the initial stage of nucleation. These nuclei have, however, different fates, depending on their size: The 3- and 4-cluster nuclei have a high probability to dismiss within a time scale of ∼20 s (i.e., time of two successive images), while the 5-cluster trapezias can easily change their conformation or reorganize into the 6-cluster quadrangle or dismiss as quickly as the 3- and 4-cluster nuclei do. Even for the 6-cluster triangles, change of conformation or subsidence into smaller unstable nuclei occurs within a time scale of ∼120 s (Figure 8b−d). In a word, these nuclei all have high probabilities to dismiss or change conformation. Only the 7-cluster hexagon-shaped nuclei can survive for a time of >200 s without subsidence or change of conformation; see, e.g., nucleus marked "2" in Figure 8e and f. Meanwhile, as other nuclei become dismissed or subsided, nuclei which contain the 7-cluster hexagon *unit* (Figure 8a−d, highlighted in thin white) continue to be formed, either completely fresh or from the reorganization of the existing unstable nuclei, which eventually unify into domains (Figure 8e and f). This evidence leads to the conclusion that the 7-cluster hexagon-shaped nuclei serve as the seeds to form stable domains. They are therefore regarded as the critical nuclei at this potential. In other words, the 7-cluster hexagon is the least stable close-packed unit under the balance of various interactions. We note that, although each of the two 7-cluster hexagons (Figure 8d and e) happens to be connected with an additional cluster, we assume that the 7-cluster hexagon itself is stable enough. Perhaps, the difficulty in finding an absolutely isolated 7-cluster hexagon already indicates its strong tendency to grow into larger domains, which serves as a proof of the stability of the 7-cluster hexagon nuclei against dissolution. It should be pointed out that nuclei without well-defined close-packed structures (such as that indicated by the black circle in Figure 8) also exist and can grow into domains, but their sizes are usually large and uncertain, depending on the actual arrangement of the clusters and strength of the resultant intermolecular interactions.

Close inspection of the close-packed yet unstable nuclei shows a common feature that there are at least two clusters which have only two nearest neighboring clusters. Subsidence or conformational change of these unstable nuclei proceeds with detachment of just these 2-coordinated clusters, which further generates new 2-coordinated clusters. Such processes could continue until complete dissolution of the nucleus. Therefore, the stability of the 7-cluster hexagon-shaped nuclei is attributed to the presence of the 6-coordinated central clusters, which makes all the six peripheral clusters 3-coordinated.

3.4.2. Escape and Recapture of Clusters. The attachment and detachment of clusters can also occur between two adjacent domains. As can be seen from a set of successively recorded STM images, Figure 9, motion of clusters prevails at the boundaries, leading to dynamic change of the domain size. However, Ostwald ripening, by which the larger island grows and the smaller one diminishes, is not observed.

Defects, where clusters are missing, exist within the domains. The vacancies thus created allow the clusters to move around (see, e.g., regions marked by white ovals). All the vacancies are stable without change of the local arrangement of the clusters. More interestingly, clusters can even escape from the area without vacancy surroundings, or insert to fill in a vacancy that may be left by the escaping cluster. This cluster on−off feature might be a consequence of the dynamic process of the electrolyte species at the interface. On the basis of a separate sequence of STM images with scan rate of 32 Hz (not shown), the cluster escape-and-recapture event taking place on the same site is estimated to be complete within 16 s in the ionic liquid, with a resolution time of 8 s of each STM image. We speculate that the escaped clusters (in fact the molecules that compose the clusters) do not diffuse away from the surface so that the probability of recapture is high.

3.4.3. Cluster Breathing. A highly interesting feature concerning the $SbCl_3$ supramolecular aggregation is the coexistence of 6-membered (central member off) and 7-membered (central member on) clusters. Close inspection of successively recorded images of the assembly structure discloses that the central member is actually also in a dynamic equilibrium. For example,

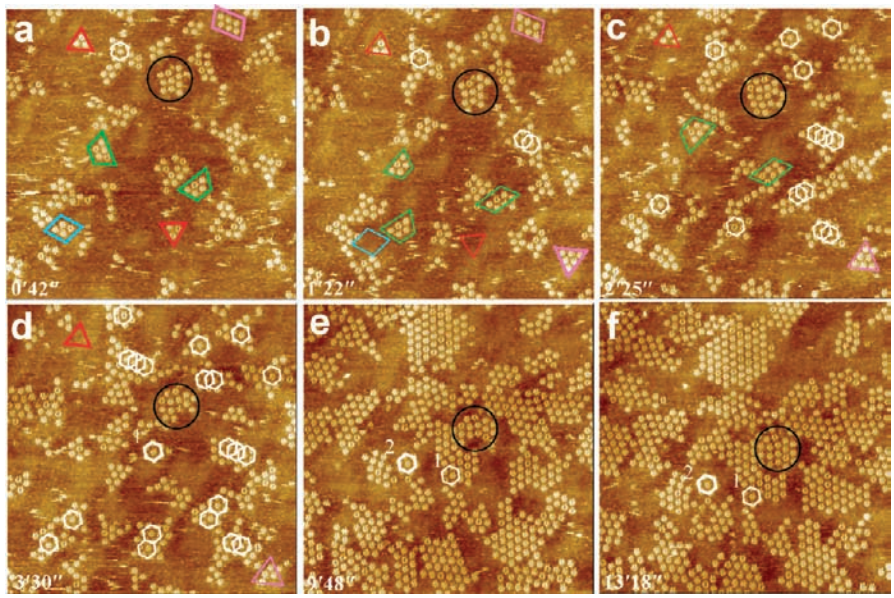

Figure 8. Sequence of STM images showing formation of $SbCl_3$ cluster domains of at 60 mV. Scan size: 50 nm × 50 nm. Tunneling current: 800 pA. Bias voltage: 100 mV.

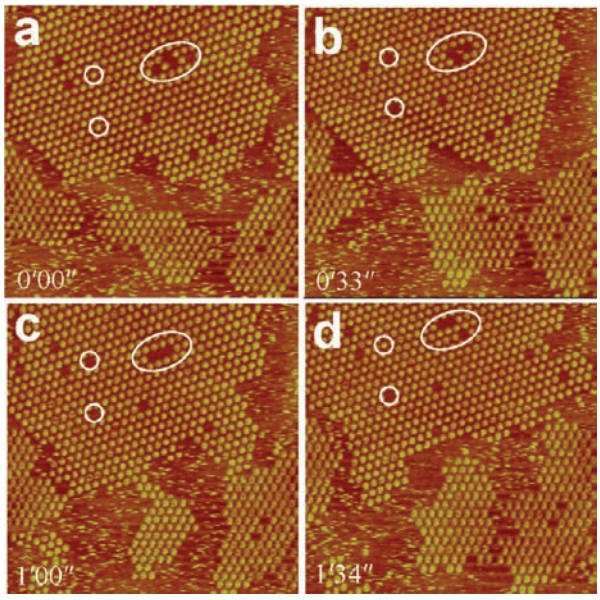

Figure 9. Escape and recapture of clusters from the assembly at 50 mV. Scan size: 50 nm × 50 nm. Tunneling current: 1 nA. Bias voltage: 250 mV.

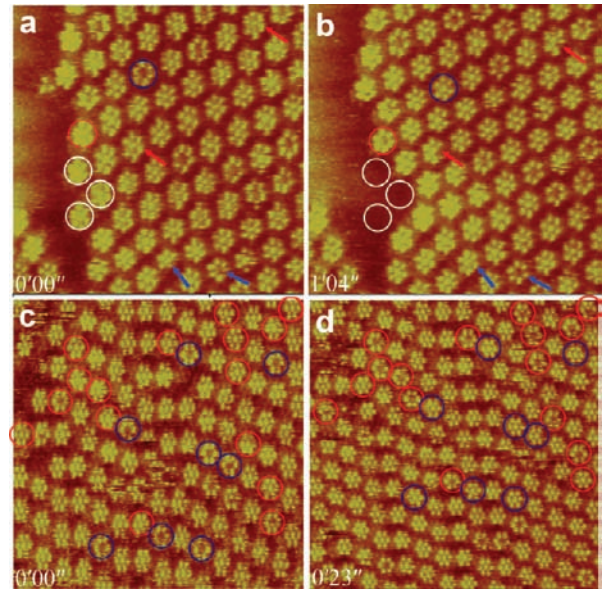

Figure 10. Successively recorded STM images showing the dynamics of central and ring members of the $SbCl_3$ clusters in (a, b) $BMIBF_4$ ionic liquid containing 0.01 M $SbCl_3$ at 0.085 V and (c, d) aqueous solution of 0.017 M $SbCl_3$ + 2 M HCl at −0.1 V. Scan size: (a, b) 15 nm × 15 nm, (c, d) 20 nm × 20 nm. (a, b) Tunneling current: 1 nA, bias voltage: 88 mV; (c, d) Tunneling current: 6 nA, bias voltage: 0.6 V.

comparing the cluster marked with the red circle in Figure 10a and 10b in ionic liquid, it is seen that the central member of the 7-membered cluster experiences an on-to-off process. Similarly, the 6-membered cluster marked with the blue circle in Figure 10a and 10b experiences an off-to-on process. The on or off event occurs with limited probability. In the ionic liquid, about 1 out of 136 clusters experiences such an on or off event with a rate of once per 5 min; while higher probability of 1 in 6 is observed in aqueous solution, Figure 10, c and d. About 50% of observed on-to-off events of the central member in ionic liquid are followed by off-to-on event within less than 16 s with a time resolution of 8 s. There are also cases in which the central member escapes or inserts but does not return or escape within the next several minutes. Unfortunately, information about the intrinsic fluctuation of the central member may be lost because of the limited time resolution of STM observation.

The members on the rings of the clusters are also found in dynamic attachment and detachment equilibrium as indicated by the blue and red arrows, respectively, in Figure 10. In most cases, only one member at the ring is involved. Similar behavior has also been observed for $BiCl_3$ in the ionic liquid. (Figure S8, Supporting Information).

The on−off process of the central members and the attaching−detaching of the ring members are regarded as cluster breathing induced by the motion of solution species. Since the clusters are partially negatively charged, the attractive Coulombic interaction with the cations from the electrolyte is indis-

pensable to stabilize the assembly. It turns out that the dynamic equilibrium of the clusters would be influenced by the properties of the cations. Imidazolium (BMI^+) and hydroxonium (H_3O^+) are the nearest cations to the clusters in the ionic liquid and concentrated HCl aqueous solutions, respectively. The strength of the attraction with the cluster is, however, insufficient to induce the coadsorption of the BMI^+ or H_3O^+, which is evident from the absence of these cations in the STM images. It is likely that the on−off process of the central members takes place when the cations temporarily deviate from the clusters, which provides the space necessary for the vertical motion of the central members. In the ionic liquid, the BMI^+ cation is sterically large, and the mobility is expected to be low. Thus, the chance for BMI^+ to deviate from the clusters would be low. In contrast, H_3O^+ in aqueous HCl solutions is much smaller yet with much higher mobility, which in turn favors the motion of the central member of clusters and thus the on−off process of the clusters. The higher fraction of the 6-member clusters and higher probability of the on−off process in concentrated HCl solutions than in $BMIBF_4$ liquid are likely the result of the higher mobility of the hydroxonium H_3O^+ at the interface.

Regardless of the detailed process, the nature of the electrolyte side of the interface can influence the dynamic equilibriums of clusters or members of the clusters in a delicate way. Especially, cations are responsible for the observed dynamic behavior. In other words, the dynamic behavior of the assembly also indirectly reflects the dynamic properties of cations at the interface.

4. Summary

In summary, we have presented a systematic study of the surface assembly of neutral inorganic molecules at electrochemical interfaces to elucidate the important roles of both potential and electrolyte on the structure and dynamics of molecular self-assembly. Our observations can be summarized as follows.

(1) The potential-induced adsorption of covalently bound semimetal types of compound molecules, $SbCl_3$ and $BiCl_3$, on a Au(111) electrode is driven by molecule−surface interactions involving partial charge transfer from the surface to the molecules. Chlorine-based, short-range, intermolecular interactions promote supramolecular aggregation of the adsorbed XCl_3. Two types of supramolecular structures are formed in the $BMIBF_4$ ionic liquid, namely the 6-membered clusters with or without the central member for both $SbCl_3$ and $BiCl_3$ and the 3-membered trigonal clusters for $BiCl_3$ only. Repulsive Coulombic interactions created between the partially charged clusters facilitate the long-range ordering of the clusters.

(2) The stability of the supramolecular clusters and their array structures relies on a subtle balance of molecule−surface, molecule−molecule, and molecule−electrolyte interactions, wherein strong ionic strength plays a crucial role. Ions in the electric double layer can provide strong attractive or repulsive Coulombic interactions with the negatively charged clusters, depending on the concentration of the electrolyte. Increasing the concentration of ClO_4^- in concentrated HCl solutions to above 2.5 M turns the attractive cluster−cation interactions into repulsive cluster−anion interactions, which prevents supramolecular aggregation. The results reveal an important principle that interactions from the solution side of the electrochemical interface cannot be overlooked when dealing with self-assembly of neutral inorganic molecules.

(3) The formation of $SbCl_3$ assemblies follows a two-dimensional nucleation and growth mechanism, and the clusters and their domains are dynamic. The dynamic equilibrium of the cluster domains is related to the surface mobility of the clusters and thus the molecule−surface interaction, while the dynamic equilibrium of clusters (i.e., escape and recapturing of clusters) and the members in the clusters (i.e., cluster breathing) is influenced in a delicate way by the nature of the cations at the electric double layer and thus by molecule−electrolyte interactions. These phenomena also indirectly reflect the dynamic properties of the cations of the media at the interface.

In conclusion, by employing semimetal types of compound inorganic molecules, molecular self-assembly has been generalized to neutral inorganic molecular systems. The rich information contained in the self-assembly of $SbCl_3$ and $BiCl_3$ convincingly shows that these molecules can serve as model systems for fundamental studies on a variety of interesting issues, especially the interplay of various interfacial interactions. Among these interactions, the significance of the electrolyte must be taken into consideration.

Acknowledgment. We are grateful to Prof. Michael Blackburn at the University of Sheffield for MS improvement. This work was supported by the NSF of China (Grants 20433040, 20673090) and the National Basic Research Program of China (973 Program; 2007CB935603).

Supporting Information Available: Further details, CVs, and EC-STM images. This material is available free of charge via the Internet at http://pubs.acs.org.

JA902373Q